Energy 79 (2015) 363–370

Contents lists available at ScienceDirect

Energy

journal homepage: www.elsevier.com/locate/energy

Ethanol adsorption onto metal organic framework: Theory and experiments

Bidyut Baran Saha [a, d, *], Ibrahim I. El-Sharkawy [b, c, d], Takahiko Miyazaki [b, d], Shigeru Koyama [a, b, d], Stefan K. Henninger [e], Annika Herbst [f], Christoph Janiak [f]

[a] Interdisciplinary Graduate School of Engineering Sciences, Kyushu University, Kasuga-koen 6-1, Kasuga-shi, Fukuoka 816-8580, Japan
[b] Faculty of Engineering Sciences, Kyushu University, Kasuga-koen 6-1, Kasuga-shi, Fukuoka 816-8580, Japan
[c] Mechanical Power Engineering Department, Faculty of Engineering, Mansoura University, El-Mansoura 35516, Egypt
[d] International Institute for Carbon-Neutral Energy Research (WPI-I2CNER), Kyushu University, 744 Motooka, Nishi-ku, Fukuoka 819-0395, Japan
[e] Fraunhofer Institute for Solar Energy Systems (ISE), Dept. Thermally Active Materials and Solar Cooling Heidenhofst, 2-79110 Freiburg, Germany
[f] Institut für Anorganische Chemie und Strukturchemie, University of Düsseldorf, Universitätsstr. 1, D-40225 Düsseldorf, Germany

A R T I C L E I N F O

Article history:
Received 17 July 2014
Received in revised form
10 October 2014
Accepted 7 November 2014
Available online 9 December 2014

Keywords:
Adsorption isotherms
Adsorption kinetics
Ethanol
Metal organic framework

A B S T R A C T

This paper presents experimental and theoretical investigations of adsorption characteristics of ethanol onto metal organic framework namely MIL-101Cr. Adsorption isotherms and kinetics of the studied pair have been measured gravimetrically using a magnetic suspension adsorption measurement unit and volumetrically employing a Quantachrome Autosorb iQ MP machine. The present experiments have been conducted within relative pressures between 0.1 and 0.9 and adsorption temperatures ranging from 30 to 70 °C, which are suitable for adsorption cooling applications. Adsorption isotherm data exhibit that 1 kg of MIL-101Cr can adsorb as high as 1.1 kg of ethanol at adsorption temperature of 30 °C, and the Tóth equation has been used to fit the experimentally measured data. As of the experimentally measured adsorption uptake rate data, the Fickian diffusion model is found to be suitable. These data are essential for designing a new generation of adsorption chiller.

1. Introduction

MOFs (Metal-organic frameworks) are materials in which metal-to-organic ligand interactions yield porous coordination networks. It is proven that the MOFs have higher surface area than activated carbons and zeolites. They are widely used in methane and hydrogen storage, gas separation and catalysis [1–9]. Moreover, extensive research efforts have been conducted recently to investigate the possible use of the MOFs in adsorption cooling applications. Following are some representative examples. Henninger et al. [10] tested the cycle stability of sorption materials and composites for possible use in heat pumps and adsorption cooling. The authors tested common materials such as silica gels and zeolites and other developed materials like aluminophosphates (AlPO), SAPO (silica aluminophosphates) and metal organic frameworks. The studied materials have been analyzed under continuous thermal cycling in a water vapor atmosphere. Jeremias et al. [11] discussed the feasibility of using the metal–organic frameworks UiO-66(Zr), UiO-67(Zr), H_2N-UiO-66(Zr) and H_2N-MIL-125(Ti) in heat transformation. Adsorption isotherms of water onto the studied types of MOFs have been presented and analyzed. Water sorption onto functionalized MIL-101Cr has also been investigated for possible use in adsorption chillers [12]. Adsorption characteristics of water into two types of MOFs has been experimentally investigated and compared with that of silica gel/water pair [13]. Aristov [14] reviewed several classes of materials potentially promising for adsorption heat transformation applications. These materials include metal aluminophosphates (AlPOs, SAPOs, MeAPOs), selected types of metal-organic frameworks, ordered porous solids,

* Corresponding author. Interdisciplinary Graduate School of Engineering Sciences, Kyushu University Program for Leading Graduate School, Green Asia Education Center, Kyushu University, Kasuga-koen 6-1, Kasuga-shi, Fukuoka 816-8580, Japan.
E-mail address: saha.baran.bidyut.213@m.kyushu-u.ac.jp (B.B. Saha).

http://dx.doi.org/10.1016/j.energy.2014.11.022
0360-5442/

Nomenclature

A	surface area of adsorbent (m^2)
b	the affinity constant presented in Eq. (2) (kPa^{-1})
b_o	the affinity at the reference temperature (kPa^{-1})
D	diffusivity ($m^2\ s^{-1}$)
D_{so}	pre-exponential constant ($m^2\ s^{-1}$)
E_a	activation energy ($kJ\ kg^{-1}$)
F	fractional uptake (–)
p	equilibrium pressure (kPa)
p_o	saturation pressure (kPa)
Q	isosteric heat of adsorption at zero fractional uptake ($kJ\ kmol^{-1}$)
R	universal gas constant ($kJ\ kmol^{-1}\ K^{-1}$)
R_g	gas constant ($kJ\ kg^{-1}\ K^{-1}$)
R_p	particle radius (m)
T	temperature (K)
T_o	reference temperature (K)
t	time (s) and parameter in Tóth isotherm (–)
V	the adsorbent particle volume (m^3)
W	equilibrium adsorption uptake ($kg\ kg^{-1}$)
w	instantaneous adsorption uptake ($kg\ kg^{-1}$)
w_{in}	initial uptake ($kg\ kg^{-1}$)
W_s	saturated adsorption capacity ($kg\ kg^{-1}$)
W_o	reference adsorption capacity ($kg\ kg^{-1}$)
φ	constant temperature of Eq. (3)

porous carbons and various composites (SWSs, AlPO–Al foil). Other studies on adsorbent/refrigerant pairs for cooling applications could be found elsewhere [15–30]. However, there is no precise analysis on the adsorption isotherm and kinetics of ethanol onto MOFs.

From the above perspectives, this study presents an experimental investigation on adsorption characteristics of MIL-101Cr + ethanol pair for adsorption cooling applications. Adsorption isotherms and kinetics of the studied pair have been measured within adsorption temperatures ranging from 30 to 70 °C and relative pressures between 0.1 and 0.9. Tóth equation is used to express the adsorption isotherm data whilst Fickian diffusion model is found to be suitable to present the adsorption kinetics.

2. Materials

2.1. Structure of MIL-101Cr

The compound MIL-101Cr, introduced by the group of Férey [31] as Material of Institute Lavoisier No. 101 is by now one of the best known and most cited MOFs. A pore volume of $V_{Pore} = 2.0\ cm^3\ g^{-1}$ and very high internal surface area of $S_{BET} = 4100 \pm 200\ m^2\ g^{-1}$ have been reported for this mesoporous chromium(III) terephthalate, calculated from N_2 adsorption isotherms.

The framework is similar to that of the MZN zeolite topology with an empirical formula $[Cr_3(O)(bdc)_3(F,OH)(H_2O)_2]$. The building blocks are benzene-1,4-dicarboxylate ligands bridging Cr_3O units thereby forming trinuclear $\{Cr_3(\mu_3\text{-}O)(O_2C\text{-})_6(F,OH)\ (H_2O)_2\}$ building units (SBUs) (see Fig. 1a). MIL-101Cr has two terminal water molecules connected to the trinuclear $\{Cr_3(\mu_3\text{-}O)\ (O_2C\text{-})_6(F,OH)\ (H_2O)_2\}$ building units with their octahedral Cr(III) ions. The trinculear units are vertices of supertetrahedra (Fig. 1b). The vertex-sharing supertetrahedra (b) then form a three-dimensional network (Fig. 1c) with two types of mesoporous cages. The small cage (Fig. 1d) has an inner diameter 29 Å and only pentagonal windows. The large cage (Fig. 1e) has an inner diameter of 34 Å and both pentagonal and hexagonal windows. The window apertures are 12 Å or 15–16 Å, respectively (Fig. 1f). MIL-101Cr crystal was obtained with octahedral crystal morphology in the range of 0.1 μm–1 μm. The SEM (scanning electron microscope) picture of MIL-101Cr is shown in Fig. 2.

2.2. Surface and pore analysis

Surface and pore analysis by nitrogen adsorption were performed on a Quantachrome Nova 3000. The nitrogen adsorption at 77.4 K shows the previously reported shape with a steep increase within low relative pressure followed by a characteristic second step at a relative pressure of approximately 0.19 p/p_0 (see Fig. 3). Surface area has been calculated to be 3318 $m^2\ g^{-1}$ using the multi-point BET (Brunauer–Emmett–Teller) approach on the adsorption path within the relative pressure range of 0.04–0.2 p/p_0. This value is significantly below the reported surface area of up to 4230 $m^2\ g^{-1}$ [32]. This is due to the purification step. As reported by Hong et al. [32], the purification has a major influence on the surface area. In the present work, BET areas of 2800 $m^2\ g^{-1}$ up to 4230 $m^2\ g^{-1}$ were reported on the same batch, with different purification means. The reported purification technique employed hot ethanol/water and aqueous ammonium fluoride (NH_4F) treatment, whereas we only washed the MOF sample within DMF (dimethyl formamide) and ethanol at room temperature without NH_4F treatment. However, the total pore volume, measured at a relative pressure $p/p_0 = 0.98$ was determined to 2.02 $cm^3\ g^{-1}$ which is in good agreement to the reported volume of up to 2.15 $cm^3\ g^{-1}$. Pore size distribution calculation by NLDFT (Non-Local Density Functional Theory) using a cylindrical pore model reveals two pores at about 10 Å and 16 Å, which are slightly lower than those estimated from the crystal structure given above [32].

3. Experimental apparatus and procedure

Adsorption isotherms and kinetics of the studied pair has been measured gravimetrically using a magnetic suspension adsorption measurement unit of type MSB-VG-S2. Fig. 4 shows a pictorial view of the magnetic suspension balance section which comprises; (i) balance to measure the weight of sample using a suspending system, (ii) magnetic coupling section which is equipped with the permanent magnet, (iii) circulation oil jacket to perform stable temperature control during the measurements, (iv) isothermal circulation oil bath, (v) sample cell, and (vi) sheathed heater to heat the sample cell. Both the magnetic coupling section and sample cell is isolated using thermal insulation. The repeatability of the weight measurements is ±30 μg with a relative error of ±0.002% of the reading. Three types of pressure gauges namely; (i) 3500 kPa, Keller PAA-35XHTT-35, (ii) 133.3 kPa, MKS 628B13TBE1B, and (iii) 13.3 kPa, MKS 628B12TBE1B with an accuracy of 0.15–0.25% FS are used for the pressure measurements. A platinum temperature element (Pt 100U) is used to control and measure the temperature of the sample section. For each isotherm, the adsorption temperature is kept constant whilst evaporator temperature is increased stepwise. Mass of dry adsorbent sample used in the present measurements is 44.8 mg. A detailed description of the experimental procedure has been presented by El-Sharkawy et al. [23].

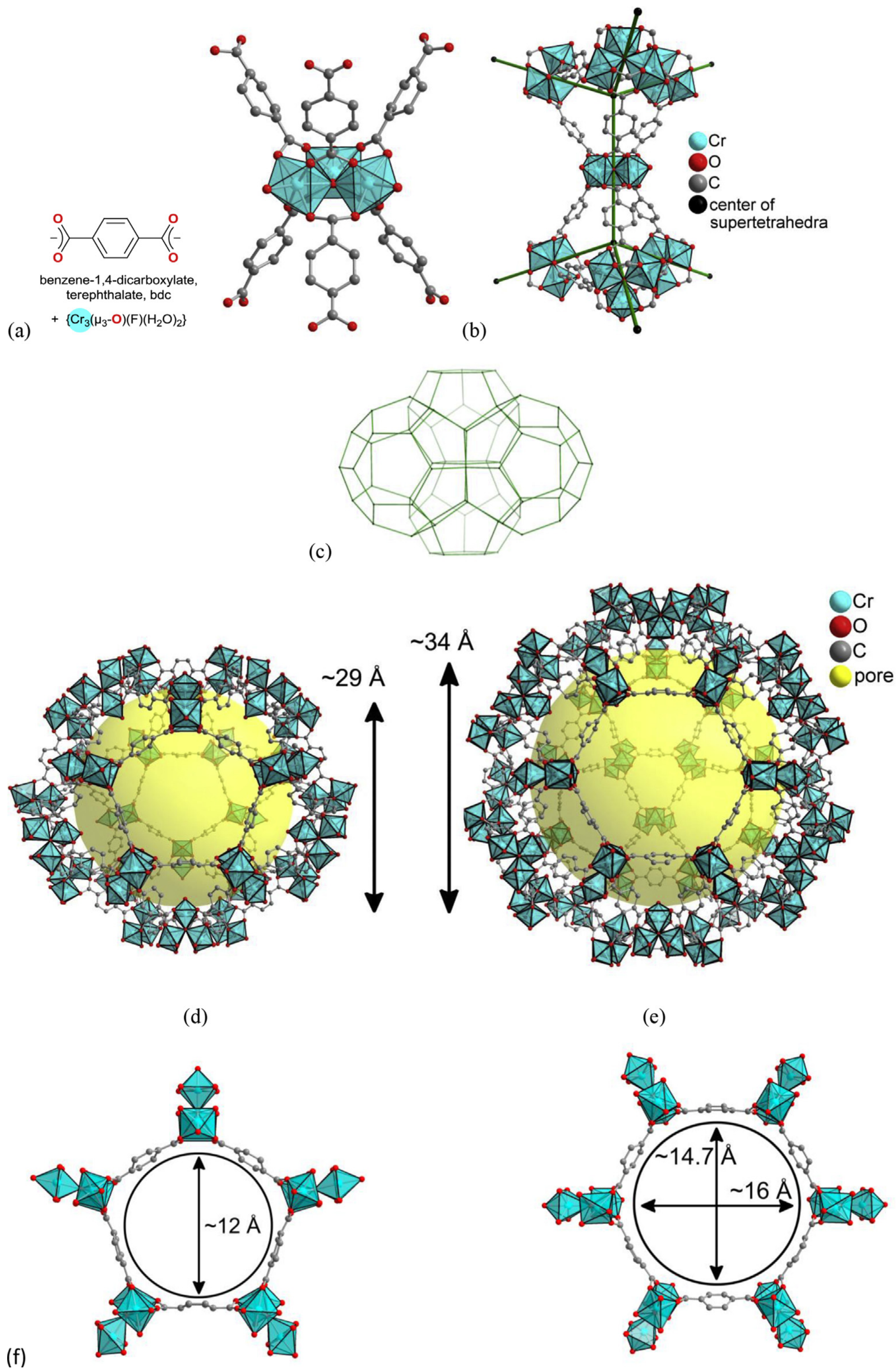

Fig. 1. (a) Ligand and metal building blocks in the trinuclear {$Cr_3(\mu_3\text{-}O)$ $(O_2C\text{-})_6$(F,OH) $(H_2O)_2$} building unit; (b) supertetrahedra; (c) mesoporous network; (d) small cage with pentagonal windows; (e) large cage with pentagonal and hexagonal windows; (f) dimensions of pentagonal and hexagonal cage window apertures. Objects in (a) to (f) are not drawn to scale. Graphics have been created from the deposited cif-file for MIL-101Cr (CSD-Refcode OCUNAK).

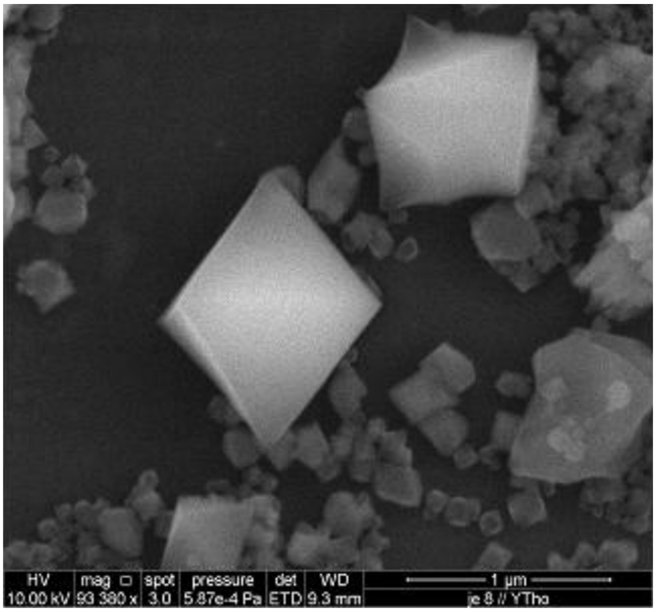

Fig. 2. The SEM picture of MIL-101Cr.
Source: Ehrenmann J, Henninger SK, Janiak C. Water adsorption characteristics of MIL-101 for heat-transformation applications of MOFs. Eur J Inorg Chem 2011:471–4.

The volumetric ethanol adsorption isotherm is measured with a Quantachrome Autosorb iQ MP instrument at a temperature of 20 °C.

4. Results and discussion

4.1. Adsorption isotherms

Fig. 5(a)–(e) shows the gravimetric adsorption isotherms of MIL-101Cr/ethanol pair for adsorption temperatures ranging from 30 to 70 °C and relative pressures between 0.1 and 0.9. For each adsorption isotherm, the adsorbent sample temperature is kept constant whilst the evaporator temperature increases stepwise until the relative pressure reaches above 0.9. It can be seen from Fig. 5(a)–(e) that, the adsorption capacity of MIL-101Cr/ethanol pair is as high as 1.1 kg kg^{-1} at adsorption temperature of 30 °C. It can be observed that, the adsorption capacity increases with the increase of relative pressure until it reaches 0.3 or 0.4. After that the increase in adsorption capacity is only marginal. Tóth equation (Eq. (1)) is used to fit the adsorption isotherms of the studied pair [33].

$$W = W_s \frac{bp}{\left[1 + (bp)^t\right]^{\frac{1}{t}}} \tag{1}$$

where;

$$b = b_o \exp\left(\frac{Q}{RT} - \frac{Q}{RT_o}\right) \tag{2}$$

$$W_s = W_o \exp\left(\varphi\left(1 - \frac{T}{T_o}\right)\right) \tag{3}$$

where W is the adsorption equilibrium uptake, W_s is the saturated adsorption capacity whilst W_o is the reference adsorption capacity. In the present study, the reference temperature is considered as 303 K. The parameters b is the affinity constant and b_o represents the affinity at the reference temperature. The term φ is a constant temperature, and Q is the measure of isosteric heat of adsorption at zero fractional uptake. Fig. 6 shows the measured adsorption isotherms and the fitting with Tóth equation. The numerical values of the Tóth parameters are enumerated in Table 1.

As reported earlier, MIL-101 shows high uptakes of organic vapors e.g. benzene or methanol [32,34]. The volumetric adsorption isotherm for ethanol onto MIL-101Cr at 20 °C is presented in Fig. 7. The very high ethanol uptake of already ~0.2 kg kg^{-1} at low relative pressure of 0.05 p/p_0 can be attributed to the CUS (co-ordinatively unsaturated metal sites). As reported by Hong et al. [32], the original present terminal water molecules at the chromium (III) cluster can be removed by heating up to 150 °C under evacuation. Thus, first strong adsorption of ethanol molecules is likely to appear at the CUS. An almost linear uptake can be observed for relative pressure up to approximately 0.35 p/p_0, corresponding to a continuous filling of the smaller cages with diameter of 29 Å (see Fig. 1d) and an additional loading of up to ~0.95 kg kg^{-1}. Following a relative pressure of 0.35 p/p_0, which may be attributed to the filling of the larger cages (see Fig. 1e), the loading finally approaching a plateau with a total uptake of 1.1 kg kg^{-1}.

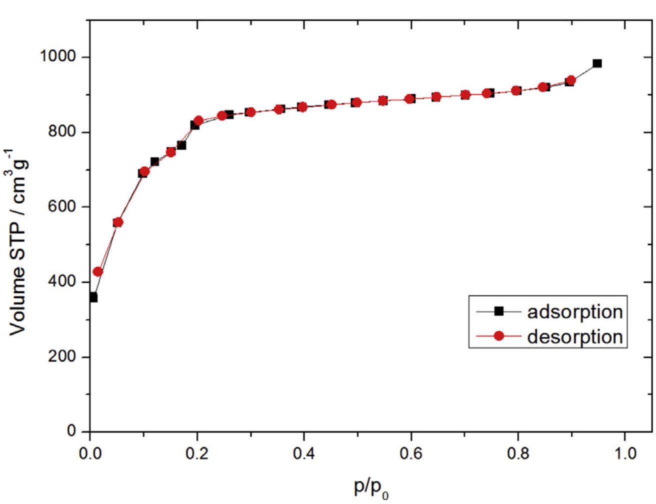

Fig. 3. Nitrogen adsorption and desorption isotherm.

4.2. Adsorption kinetics

Figs. 8 and 9 show the temporal profiles of adsorption uptake and pressure of the studied pair at adsorption temperatures of 30 and 70 °C, respectively. It is visible that, adsorption kinetics of the studied pair is relatively faster at the early stages of adsorption processes. To estimate the adsorption uptake rate of spherical shape adsorbent the following differential equation [35] can be used.

$$\frac{\partial w}{\partial t} = \frac{1}{r^2}\frac{\partial}{\partial r}\left(r^2 D \frac{\partial w}{\partial r}\right) \tag{4}$$

Solution of Eq. (4) is given by Eq. (5) below [36];

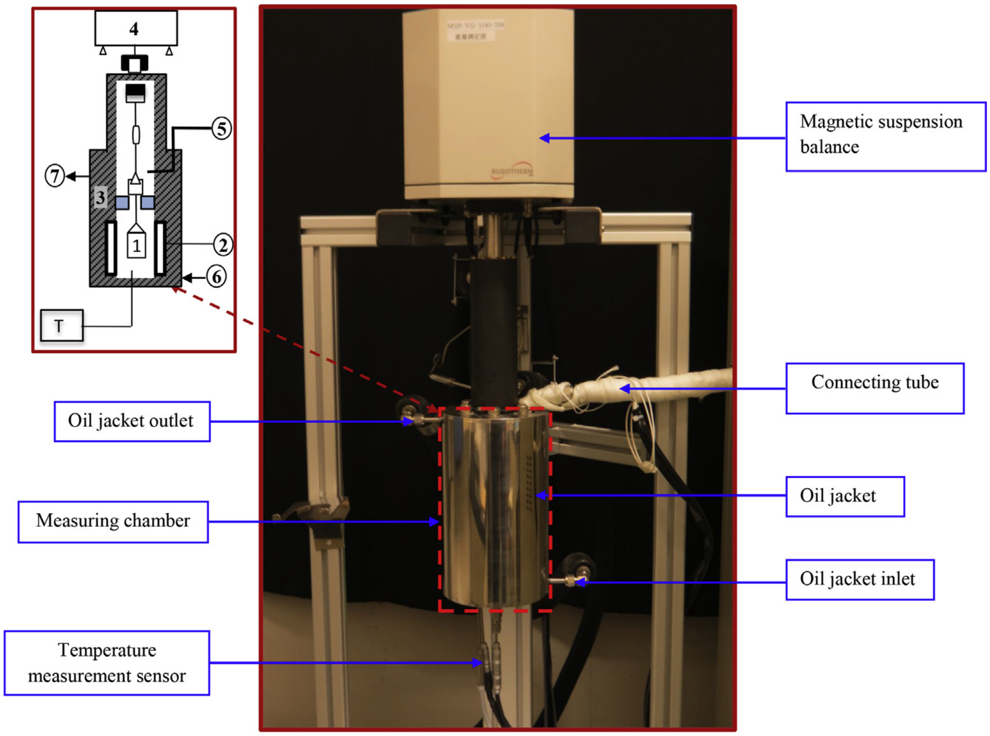

1. Sample cell; 2. Sheathed heater; 3. Circulation oil jacket; 4. Magnetic suspension balance; 5. Connecting tube; 6. Oil jacket inlet; 7. Oil jacket outlet; T:Thermocouple.

Fig. 4. Pictorial view of magnetic suspension balance section.

$$F = \frac{w - w_{in}}{W - w_{in}} = 1 - \frac{6}{\pi^2}\sum_{n=1}^{\infty}\frac{1}{n^2}\exp\left(-\frac{n^2\pi^2 Dt}{R_p^2}\right) \tag{5}$$

During the initial phase of adsorption, the diffusion time constant (D/R_p^2) can be assessed using Eq. (6) below [35];

$$F \approx \frac{2A}{V}\left(\frac{Dt}{\pi}\right)^{\frac{1}{2}} \tag{6}$$

In Eq. (6), the right hand side presents the fractional uptake, A is the surface area of adsorbent and V is the adsorbent particle volume. Eq. (6) can be simplified as given below;

$$F \approx \frac{6}{\sqrt{\pi}}\sqrt{\frac{D}{R_p^2}t} \tag{7}$$

Using Eq. (7), the diffusion time constant (D/R_p^2) is evaluated for each adsorption step. It is found that, the estimated diffusion time constant of MIL-101Cr/ethanol pair provides underestimation of adsorption uptake for all adsorption isotherms. Therefore, a diffusion time constant correction factor of 1.2 is used at all adsorption isotherms. Fractional uptake plots of experimental versus Fickian diffusion model for certain adsorption steps are shown in Fig. 10. One can see from Fig. 10 that, the maximum percentage of deviation is about ±13%.

The average values of the diffusion time constant of the first three steps are estimated (see Table 2) and the plot of $\ln(D/R_p^2)$ versus $(1/T)$ is presented in Fig. 11. Numerical values of the activation energy E_a and the pre-exponent constant (D_{so}/R_p^2) are predicted using the Arrhenius equation given below;

$$D = D_{so}\exp\left(\frac{-E_a}{R_g T}\right) \tag{8}$$

The diffusion time constant varies with $(1/T)$ according to the following expression;

$$\ln\left(\frac{D}{R_p^2}\right) = \ln\left(\frac{D_{so}}{R_p^2}\right) - \left(\frac{E_a}{R_g}\right)\left(\frac{1}{T}\right) \tag{9}$$

Experimental results show that the numerical values of E_a and (D_{so}/R_p^2) are 770 kJ kg^{-1} and 404 s^{-1}, respectively. One can notice that the activation energy of MIL-101Cr/ethanol pair is significantly higher than that of other activated carbons/ethanol pairs [23]. It can be noticed that the diffusion time constant of the studied pair has stronger dependency on adsorption temperatures in comparison with that of the carbon based adsorbents + ethanol pairs.

5. Conclusions

Adsorption isotherms and kinetics of MIL-101Cr/ethanol pair has been measured gravimetrically using a magnetic suspension adsorption measurement instrument and volumetrically

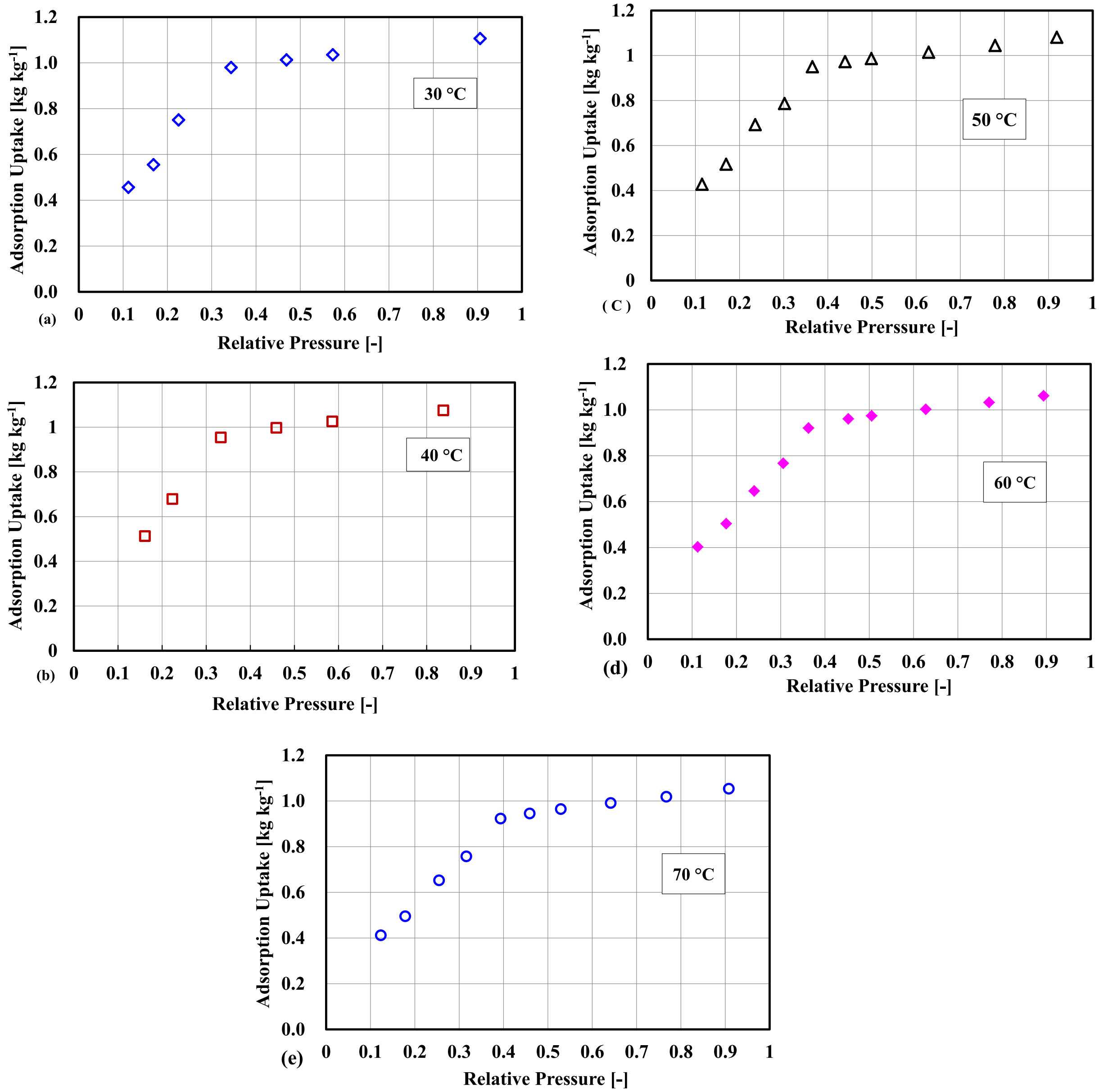

Fig. 5. Gravimetric adsorption isotherms of MIL-101Cr/ethanol pair.

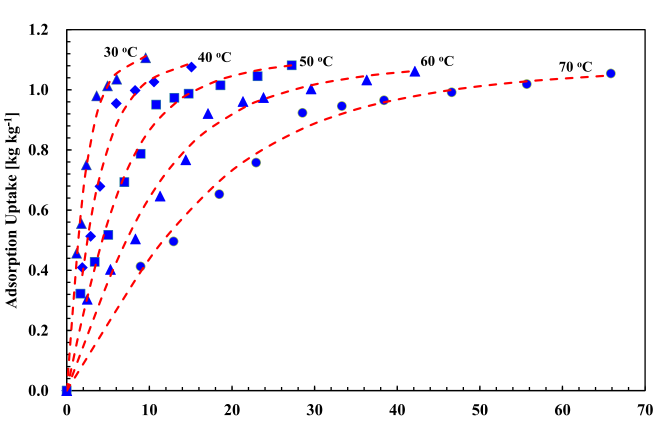

Fig. 6. Adsorption isotherms using Tóth equation (symbols: experiments; Tóth fitting using all temperature range: dashed lines).

employing a Quantachrome Autosorb iQ MP machine. Experimental results show that the assorted adsorbent, MIL-101Cr, can adsorb up to 1.1 kg of ethanol per kg of dry adsorbent. The Tóth adsorption isotherm model is used to fit the adsorption equilibrium uptake of the studied pair whilst the Fickian diffusion model is used to represent adsorption kinetics. It is found that the diffusion time constant of the studied pair strongly depends on adsorption temperatures. Experimental results show that the studied pair would be a promising candidate for developing high performance cooling device.

Table 1
Parameters of Tóth isotherms model.

Tóth parameters covering adsorption temperature from 30 to 70 °C					
Temperature [°C]	W_o	b_o	t	Q/RT_o	φ
30–70	1.150	0.342	2.193	17.845	0.358

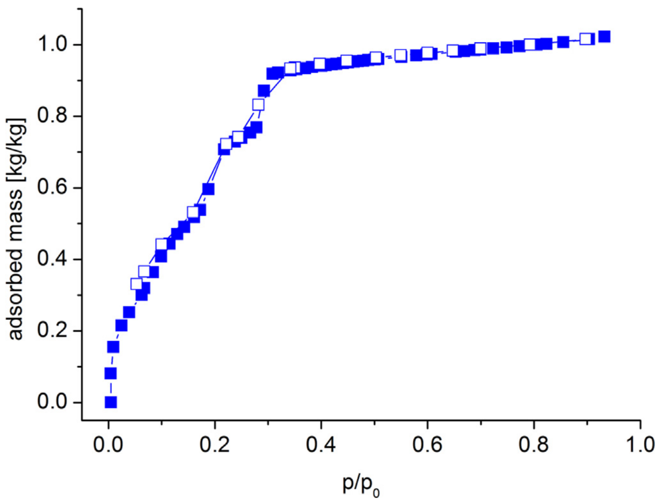

Fig. 7. Volumetric sorption isotherm of MIL-101Cr/ethanol pair at 20 °C. The closed and open symbols refer to adsorption and desorption, respectively.

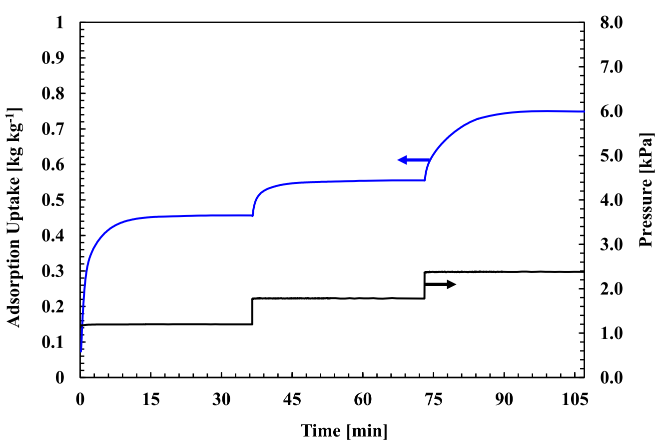

Fig. 8. Plots of adsorption uptake and pressure versus time for MIL-101Cr/ethanol pair at adsorption temperature of 30 °C.

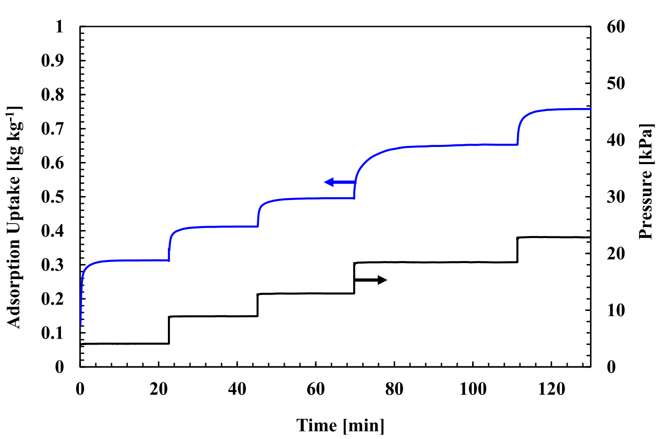

Fig. 9. Plots of adsorption uptake and pressure versus time for MIL-101Cr/ethanol pair at adsorption temperature of 70 °C.

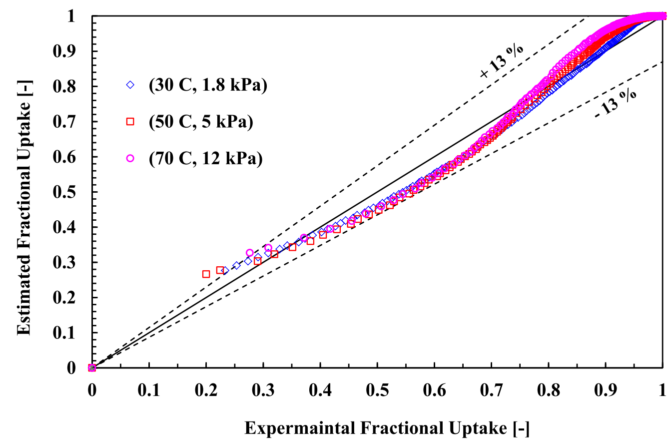

Fig. 10. Plots of adsorption uptake and pressure versus time for MIL-101Cr/ethanol pair at adsorption temperature of 70 °C.

Table 2
Numerical values of diffusion time constant of MIL-101Cr/ethanol pair.

T_{ads}, [°C]	Equilibrium pressure, [kPa]	D/R_p^2 [s^{-1}]
30.0	1.19	4.50×10^{-4}
	1.78	3.61×10^{-4}
	2.38	1.08×10^{-4}
40.1	1.89	7.76×10^{-4}
	2.89	5.17×10^{-4}
	4.03	1.67×10^{-4}
49.9	1.66	1.03×10^{-3}
	3.41	7.58×10^{-4}
	5.03	6.52×10^{-4}
60.0	2.47	1.47×10^{-3}
	5.30	1.13×10^{-3}
	8.33	8.83×10^{-4}
69.9	4.07	2.25×10^{-3}
	8.94	1.35×10^{-3}
	12.94	1.02×10^{-3}

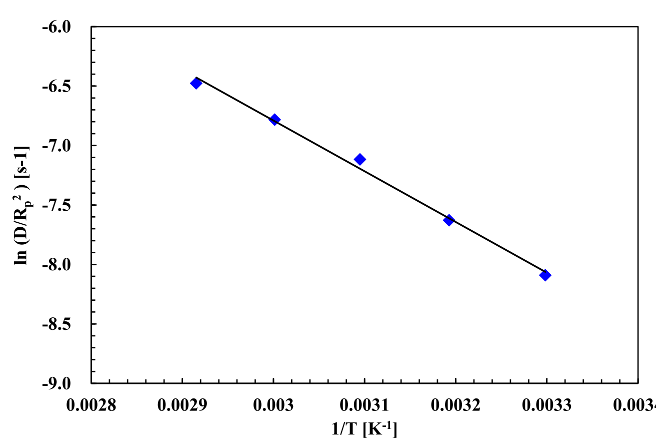

Fig. 11. Arrhenius plot of MIL-101Cr/ethanol pair.

Acknowledgments

This work was financially supported by Japan Science and Technology Agency (JST), Core Research for Evolutional Science and Technology (CREST).

References

[1] Murray LJ, Dinca M, Long JR. Hydrogen storage in metal-organic frameworks. Chem Soc Rev 2009;38(5):1294–314.
[2] Saha D, Wei Z, Deng S. Equilibrium, kinetics and enthalpy of hydrogen adsorption in MOF-177. Int J Hydrogen Energy 2008;33(24):7479–88.
[3] Sanz R, Martinez F, Orcajo G, Wojtas L, Briones D. Synthesis of a honeycomb-like Cu-based metal-organic framework and its carbon dioxide adsorption behaviour. Dalton Trans 2013;42(7):2392–8.
[4] Munusamy K, Sethia G, Patil DV, Somayajulu Rallapalli PB, Somani RS, Bajaj HC. Sorption of carbon dioxide, methane, nitrogen and carbon monoxide on MIL-101(Cr): volumetric measurements and dynamic adsorption studies. Chem Eng J 2012;195-196:359–68.
[5] Li J-R, Ma Y, McCarthy MC, Sculley J, Yu J, Jeong H-K, et al. Carbon dioxide capture-related gas adsorption and separation in metal-organic frameworks. Coord Chem Rev 2011;255(15–16):1791–823.
[6] Henschel A, Gedrich K, Kraehnert R, Kaskel S. Catalytic properties of MIL-101. Chem Commun (Camb) 2008;35:4192–4.
[7] Li Y, Yang RT. Gas adsorption and storage in metal-organic framework MOF-177. Langmuir 2007;23(26):12937–44.
[8] Llewellyn PL, Bourrelly S, Serre C, Vimont A, Daturi M, Hamon L, et al. High uptakes of CO_2 and CH_4 in mesoporous metal-organic frameworks MIL-100 and MIL-101. Langmuir 2008;24(14):7245–50.
[9] Lin RB, Chen D, Lin YY, Zhang JP, Chen XM. A zeolite-like zinc triazolate framework with high gas adsorption and separation performance. Inorg Chem 2012;51(18):9950–5.
[10] Henninger SK, Munz G, Ratzsch KF, Schossig P. Cycle stability of sorption materials and composites for the use in heat pumps and cooling machines. Renew Energy 2011;36(11):3043–9.
[11] Jeremias F, Lozan V, Henninger SK, Janiak C. Programming MOFs for water sorption: amino-functionalized MIL-125 and UiO-66 for heat transformation and heat storage applications. Dalton Trans 2013;42(45):15967–73.
[12] Khutia A, Rammelberg HU, Schmidt T, Henninger S, Janiak C. Water sorption cycle measurements on functionalized MIL-101Cr for heat transformation application. Chem Mater 2013;25(5):790–8.
[13] Rezk A, Al-Dadah R, Mahmoud S, Elsayed A. Characterisation of metal organic frameworks for adsorption cooling. Int J Heat Mass Transfer 2012;55(25–26): 7366–74.
[14] Aristov YI. Challenging offers of material science for adsorption heat transformation: a review. Appl Therm Eng 2013;50(2):1610–8.
[15] Henninger SK, Habib HA, Janiak C. MOFs as adsorbents for low temperature heating and cooling applications. J Am Chem Soc 2009;131(8):2776–7.
[16] Henninger SK, Jeremias F, Kummer H, Schossig P, Henning H-M. Novel sorption materials for solar heating and cooling. Energy Procedia 2012;30: 279–88.
[17] Henninger SK, Schmidt FP, Henning HM. Water adsorption characteristics of novel materials for heat transformation applications. Appl Therm Eng 2010;30(13):1692–702.
[18] Wickenheisser M, Jeremias F, Henninger SK, Janiak C. Grafting of hydrophilic ethylene glycols or ethylenediamine on coordinatively unsaturated metal sites in MIL-100(Cr) for improved water adsorption characteristics. Inorg Chim Acta 2013;407:145–52.
[19] Rezk A, Al-Dadah R, Mahmoud S, Elsayed A. Investigation of ethanol/metal organic frameworks for low temperature adsorption cooling applications. Appl Energy 2013;112:1025–31.
[20] Aristov YI, Restuccia G, Cacciola G, Parmon VN. A family of new working materials for solid sorption air conditioning systems. Appl Therm Eng 2002;22(2):191–204.
[21] Follin S, Goetz V, Guillot A. Influence of microporous characteristics of activated carbons on the performance of an adsorption cycle for refrigeration. Ind Eng Chem Res 1996;35(8):2632–9.
[22] Saha BB, El-Sharkawy II, Habib K, Koyama S, Srinivasan K. Adsorption of equal mass fraction near an azeotropic mixture of pentafluoroethane and 1,1,1-trifluoroethane on activated carbon. J Chem Eng Data 2008;53(8):1872–6.
[23] El-Sharkawy II, Uddin K, Miyazaki T, Saha BB, Koyama S, Miyawaki J, et al. Adsorption of ethanol onto parent and surface treated activated carbon powders. Int J Heat Mass Transfer 2014;73:445–55.
[24] Gordeeva LG, Aristov YI. Composite sorbent of methanol “LiCl in mesoporous silica gel” for adsorption cooling: dynamic optimization. Energy 2011;36(2): 1273–9.
[25] El-Sharkawy II, Hassan M, Saha BB, Koyama S, Nasr MM. Study on adsorption of methanol onto carbon based adsorbents. Int J Refrig 2009;32(7):1579–86.
[26] Saha BB, Jribi S, Koyama S, El-Sharkawy II. Carbon dioxide adsorption isotherms on activated carbons. J Chem Eng Data 2011;56(5):1974–81.
[27] Cui Q, Tao G, Chen H, Guo X, Yao H. Environmentally benign working pairs for adsorption refrigeration. Energy 2005;30(2–4):261–71.
[28] Gordeeva L, Aristov Y. Novel sorbents of ethanol “salt confined to porous matrix” for adsorptive cooling. Energy 2010;35(6):2703–8.
[29] Chakraborty A, Leong KC, Thu K, Saha BB, Ng KC. Theoretical insight of adsorption cooling. Appl Phys Lett 2011;98(22):221910.
[30] Sun B, Chakraborty A. Thermodynamic formalism of water uptakes on solid porous adsorbents for adsorption cooling applications. Appl Phys Lett 2014;104(20):201901.
[31] Férey C, Mellot-Draznieks C, Serre C, Millange F, Dutour J, Surblé S, et al. Chemistry: a chromium terephthalate-based solid with unusually large pore volumes and surface area. Science 2005;309(5743):2040–2.
[32] Hong DY, Hwang YK, Serre C, Férey G, Chang JS. Porous chromium terephthalate MIL-101 with coordinatively unsaturated sites: surface functionalization, encapsulation, sorption and catalysis. Adv Funct Mater 2009;19(10): 1537–52.
[33] Do DD. Adsorption analysis: equilibria and kinetics. Imperial College Press; 1998.
[34] Jeremias F, Frohlich D, Janiak C, Henninger SK. Water and methanol adsorption on MOFs for cycling heat transformation processes. New J Chem 2014;38(5):1846–52.
[35] Ruthven DM. Principles of adsorption and adsorption processes. New York: Wiley; 1984.
[36] Crank J. Mathematics of diffusion. London: Oxford University Press; 1956.